Theoretical analysis of opening-up vesicles with single and two holes

Umeda, Tamiki
Suezaki, Yukio
Takiguchi, Kingo
Hotani, Hirokazu

(Citation)
Physical Review E,71(1):11913-11913

(Issue Date)
2005-01-31

(Resource Type)
journal article

(Version)
Version of Record

(URL)
https://hdl.handle.net/20.500.14094/90000251

Theoretical analysis of opening-up vesicles with single and two holes

Tamiki Umeda
Faculty of Maritime Sciences, Kobe University, Fukae-minami-machi, Higashinada-ku, Kobe 658-0022, Japan

Yukio Suezaki
Faculty of Medicine, Saga University, Nabeshima 5-1-1 Saga 849-8501, Japan

Kingo Takiguchi and Hirokazu Hotani
Department of Molecular Biology, Graduate School of Science, Nagoya University, Furo-cho, Chikusa-ku, Nagoya 464-8602, Japan
(Received 18 June 2004; revised manuscript received 6 October 2004; published 31 January 2005)

Cuplike lipid vesicles with a single hole and tubelike vesicles with two holes were theoretically analyzed by taking into account the line tension of membrane holes and the bending energy of membranes, using the area difference elasticity model. We numerically solved the Euler-Lagrange equation and the boundary conditions holding on the membrane edge to obtain axisymmetric vesicle shapes that minimize the total energy. The numerical results showed that when the line tension is very low, and for appropriate values of the relaxed area difference between the two monolayers of bilayer membranes, the model yields cup-, tube-, and funnel-shaped vesicles that closely resemble previously observed shapes of opening-up vesicles with additive guest molecules such as the protein talin and some detergents. This strongly suggests that these additive molecules greatly reduce the line tension of lipid membranes. The effect of the Gaussian bending modulus on the shape of the opening-up vesicles was also evaluated and the effect is greatest when the size of hole is small.

DOI: 10.1103/PhysRevE.71.011913 PACS number(s): 87.16.Dg, 82.70.Uv

I. INTRODUCTION

Lipid bilayer membranes have been studied extensively due to their importance in many areas such as biomembranes, the food industry, drug delivery, and so on. Usually, lipid bilayer membranes of single lipid components form closed vesicles in aqueous solution with appropriate boundary and initial conditions (reviews in [1]). Since exposure of the hydrophobic portion of the sheets to water creates high energy costs, no tears or holes were usually formed in the lipid membrane. To keep a closed vesicle form is important for biological cells, particularly for physiological functions.

Recent studies have shown, however, that some chemical agents such as the submembranous protein talin [2] or detergents [3] are capable of inducing a stable hole or holes in lipid membranes so that the membranes transform into cup-shaped vesicles, tubelike shapes, or lipid bilayer sheets. Although a precise mechanism has not yet been clarified, melittin (a bee toxin) causes hemolysis, and therefore the addition of melittin may make a hole in lipid bilayer membranes [4]. Here we investigate theoretically how these shapes are formed based on the principle of energy minimization.

The opening of a hole in a lipid membrane to elucidate the physical properties of biological membranes or to utilize lipid vesicles as carriers for drug or DNA delivery has proven to be a challenging task. A variety of physical techniques, such as electroporation [5], osmotic shock [6], optical tweezers [7], and adhesion [8], have been developed to open transient holes in membranes. These holes have been interpreted as the result of a mechanical balance between the membrane tension and the line tension, the free energy cost per unit length of the edges of the holes. By taking the line tension energy on a small, circular hole in a spherical vesicle, one can show that a quasistable hole opens in the membrane under the excess of inner pressure [9]. However, this model can only explain the transient holes, because the leaking out of water through the holes may reduce the pressure difference across the membranes [10]. In other example of holes, electric field and charges play an essential role in their stability [11]. However, researchers in this field have generally assumed a very small hole opened in a spherical membrane, and the model is not applicable to large deformations. For the cuplike vesicle formation of lipid and talin systems, Suezaki and others clarified the origin of the shape change of cuplike vesicle using the adsorption isotherm of talin between the periphery of the cuplike vesicle and the aqueous solvent [12]. However, the vesicle shape was estimated qualitatively as a partial sphere.

In this paper, we study the shape of the opening-up membranes, based on the idea of bending energy, which was first proposed by Helfrich [13] and has been successfully used for explaining the shape transformations of closed vesicles [1]. Membranes are assumed to have bending energy determined by the local curvatures of the surfaces. We also incorporated the nonlocal bending energy resulting from the elasticity of the area difference between the two monolayers of bilayer membranes [14]. By applying the variational method to the total energy that comprises the local and nonlocal bending energies and the line tension energy, we can derive the Euler-Lagrange equation for the membrane shape and the boundary conditions holding on the membrane edge. Recently, Tu and Ou-Yang [15] derived the shape equation and boundary conditions for the spontaneous curvature model. We apply these equations to our model. By assuming axisymmetric deformations, we numerically solve the equations to seek out the equilibrium shapes. The results show that the shapes observed in experiments are realized when the line tension and the relaxed area difference are appropriately chosen.

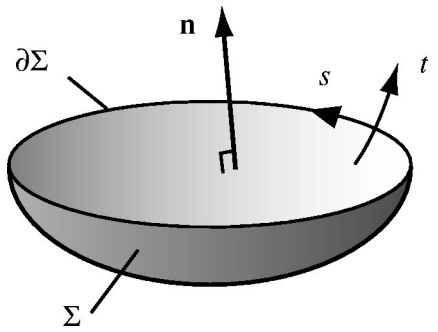

FIG. 1. The orientations of an opening-up surface and the perimeter.

II. MODEL

A. Free energy

We represent an opening-up vesicle as a two-dimensional surface Σ bordered by a closed curve (or curves) $\partial\Sigma$. To choose the direction, we take the inward normal to the membrane as positive. The perimeter $\partial\Sigma$ is oriented in the direction of the right-hand fingers if the thumb of the right hand indicates the positive normal (Fig. 1).

The energy of the membrane is the sum of three terms $F=F_c+F_r+F_\gamma$, the local bending energy of the membrane (F_c), the nonlocal bending energy of the membrane (F_r), and the line tension energy stored on the boundary $\partial\Sigma$(F_γ). The local bending energy is written as

$$F_c \equiv \int\int_\Sigma \left[\frac{k_c}{2}(2H)^2 + k_g K\right] dA, \tag{1}$$

where dA is the area element on the surface, and $H=(1/2)(1/R_1+1/R_2)$ and $K=1/R_1R_2$ are the mean and Gaussian curvatures (R_1 and R_2 are the principal curvature radii) [13]. The sign of the mean curvature is positive when vesicles assume a spherical surface. The local bending modulus k_c and the Gaussian bending modulus k_g describe the elastic properties of the membrane. The spontaneous curvature of the membrane is zero, because the two sides of an opening-up membrane are chemically identical.

The nonlocal bending energy

$$F_r \equiv \frac{k_r}{2}\frac{\pi}{AD^2}(\Delta A - \Delta A_0)^2 \tag{2}$$

stems from the relative surface dilation of the two monolayers [14]. The area difference between the two monolayers $\Delta A \equiv A^{out}-A^{in}$ is given by

$$\Delta A = 2D\int\int_\Sigma H\, dA, \tag{3}$$

where D is the distance between the two monolayers. The corresponding relaxed value $\Delta A_0 \equiv A_0^{out}-A_0^{in}$ is determined by the numbers of lipid molecules constituting the layers. The constant k_r is the nonlocal bending modulus, whose value can be estimated to be of the same order as the local bending modulus k_c [16].

Finally, the line tension energy F_γ is given by

$$F_\gamma \equiv \int_{\partial\Sigma} \gamma\, ds, \tag{4}$$

where γ is the line tension and ds the line element along $\partial\Sigma$.

B. Shape equation and boundary conditions

The equilibrium shape of the surface is obtained by minimizing F for fixed area $A=\int\int_\Sigma dA$. If the length is normalized with $R_0=(A/4\pi)^{1/2}$, the nondimensional energy $\hat{F}=F/k_c$ becomes

$$\hat{F} = \int\int_\Sigma [2H^2 + \hat{k}_g K]dA + \frac{\hat{k}_r}{2}(m-m_0)^2 + \int_{\partial\Sigma}\hat{\gamma}\, ds, \tag{5}$$

where

$$m \equiv \int\int_\Sigma H\, dA \tag{6}$$

and

$$\hat{k}_g \equiv k_g/k_c, \quad \hat{k}_r \equiv k_r/k_c,$$

$$\hat{\gamma} \equiv \gamma R_0/k_c, \quad m_0 \equiv \frac{\Delta A_0}{2DR_0}. \tag{7}$$

The surface area is now fixed at 4π, and there are four independent parameters $\hat{k}_g$, $\hat{k}_r$, $\hat{\gamma}$, and m_0 in the model.

The shape equation and the boundary conditions for opening-up vesicles are derived from the variation

$$\delta G \equiv \delta(\hat{F} + \lambda A) = 0, \tag{8}$$

where λ is the Lagrange multiplier. Equation (8) leads to the following Euler-Lagrange equation holding on the surface:

$$\Delta H + 2H(H^2 - K) + c_0 K - \lambda H = 0, \tag{9}$$

where Δ represents the Laplace-Beltrami operator on the surface and c_0 is a constant given by

$$c_0 = (\hat{k}_r/2)(m_0 - m). \tag{10}$$

This equation is the same shape equation for closed vesicles obtained by Ou-Yang and Helfrich [17] for the spontaneous curvature model except that no pressure term is involved. The constant c_0 corresponds to the spontaneous curvature of the spontaneous curvature model.

The boundary conditions for Eq. (9) are also derived from Eq. (8) using the method described in [15]. We introduce a local orthogonal frame (t,s) on the surface along the boundary $\partial\Sigma$ such that s is along $\partial\Sigma$ (Fig. 1). The boundary conditions on $\partial\Sigma$ are then

$$2H - c_0 + \hat{k}_g c_n = 0, \tag{11}$$

$$2\frac{\partial H}{\partial t} + \hat{k}_g \frac{d\tau}{ds} + \hat{\gamma} c_n = 0, \tag{12}$$

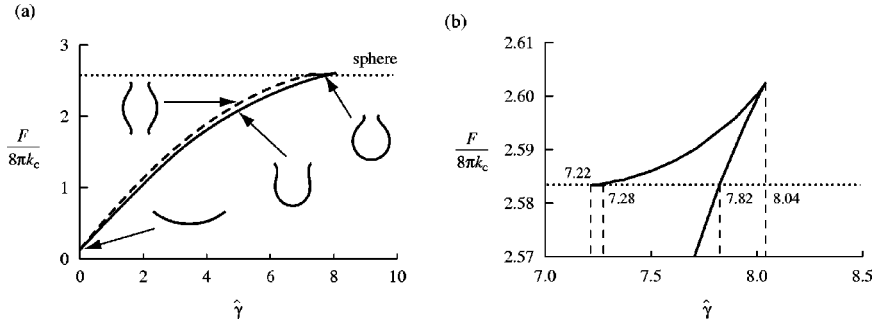

FIG. 2. The deformation of an opening-up surface when $m_0/4\pi=0.4$. (a) Energies of equilibrium shapes with one hole (solid line) and with two holes (dashed line) as functions of the normalized line tension $\hat{\gamma}=\gamma R_0/k_c$. Dotted line represents the energy of a sphere that has the same area. The figure also shows typical shapes of the surface with one hole ($\hat{\gamma}=0.0, 5.0, 7.82$) and the surface with two holes ($\hat{\gamma}=5.0$). (b) Magnification of (a) in the neighborhood of $\hat{\gamma}=7.8$. Only the energy of the surface with one hole is shown.

$$2H(H-c_0)+\hat{k}_g K+\lambda+\hat{\gamma}c_g=0, \tag{13}$$

where c_n is the normal curvature, c_g the geodesic curvature, and τ the geodesic torsion along $\partial\Sigma$. Physically, Eqs. (11) and (12) correspond to the balance of torque and the balance of shear force per unit length of the boundary, respectively. Equation (13) is associated with membrane tension. Note that the parameters $\hat{\gamma}$ and $\hat{k}_g$ are involved only in the boundary conditions.

The equilibrium shape of opening-up vesicles is obtained by solving Eq. (9) with the boundary conditions (11)–(13) and the constraints (10) and $A=4\pi$.

III. RESULTS

A. Axisymmetric deformation

We hereafter restrict our analysis to axisymmetric deformation. There are three topological types of axisymmetric surfaces: closed surfaces, surfaces with one hole, and surfaces with two holes. Shape transformations of closed vesicles have been thoroughly studied and it is known that the shape depends on the volume of water enveloped in the vesicles [18]. However, in the case of no volume constraint (in other words, no pressure term), spherical vesicles are stable if $c_0=(\hat{k}_r/2)(m0-4\pi)<6$ [13]. Thus, we may assume that closed surfaces are spherical in this range. The shape equations and the boundary conditions for axisymmetric surfaces with holes are described in Appendix A. The equations were solved using the method described in Appendix B. Although there are four independent parameters in the model, as stated previously, we fixed $\hat{k}_r$ at 1.4 according to the estimation for stearoyl-oleoyl-phosphatidylcholine (SOPC) by Miao *et al.* [14]. Furthermore, we assume $\hat{k}_g=0$ in the following three subsections. In Sec. III E, we examine the effect of the Gaussian curvature modulus on the vesicle shape. Finally, we describe the result of a minimal model in which the nonlocal bending energy is completely relaxed.

B. Surface with one hole

Figure 2 shows the deformation of opening-up surfaces when $m_0/4\pi=0.4$. Shapes with one hole bifurcate from a sphere at $\hat{\gamma}=7.28$, in which an infinitesimal hole opens in a spherical surface. The graph of energy versus line tension folds at $\hat{\gamma}=7.22$ and 8.04 so that there are three branches in the graph: $7.22\leqslant\hat{\gamma}\leqslant7.28$, $7.22\leqslant\hat{\gamma}\leqslant8.04$, and $0\leqslant\hat{\gamma}\leqslant8.04$. Shapes in the third branch vary from a cup shape to a dish shape, and they have lower energy than the shapes in the other branches at the same $\hat{\gamma}$. Moreover, they have lower energy than the sphere when $\hat{\gamma}<7.82$. Therefore, a spherical vesicle is expected to transform discontinuously into a cup shape at $\hat{\gamma}=7.82$. After that, the cup continuously changes its shape to become a dish as $\hat{\gamma}$ decreases.

C. Surface with two holes

In addition to the cup shapes, there exists another family of solutions in which two holes open at both ends of a surface. When $m_0/4\pi=0.4$, the shapes have higher energy than the cup shapes as shown in Fig. 2(a), which suggests that the shapes with two holes are unstable. However, when $m_0/4\pi=1.0$, the energy becomes lower than that of the cup shapes (Fig. 3). Shapes with two holes bifurcate from a sphere at

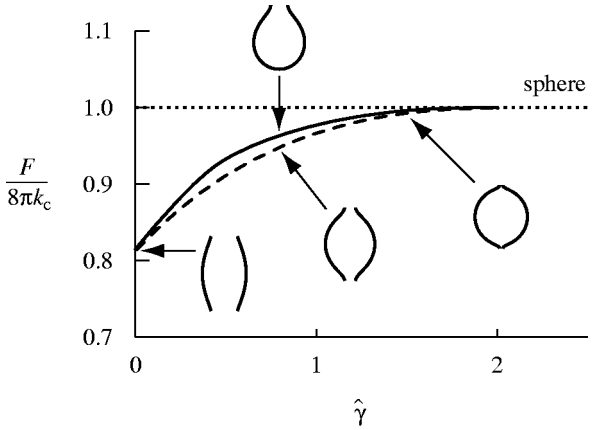

FIG. 3. The deformation of opening-up surfaces when $m_0/4\pi=1.0$. Energies of equilibrium shapes with one hole (solid line) and with two holes (dashed line) are shown against the normalized line tension $\hat{\gamma}=\gamma R_0/k_c$. Typical shapes of the surface with one hole ($\hat{\gamma}=0.8$) and the surface with two holes ($\hat{\gamma}=0.0, 0.8, 1.5$) are depicted.

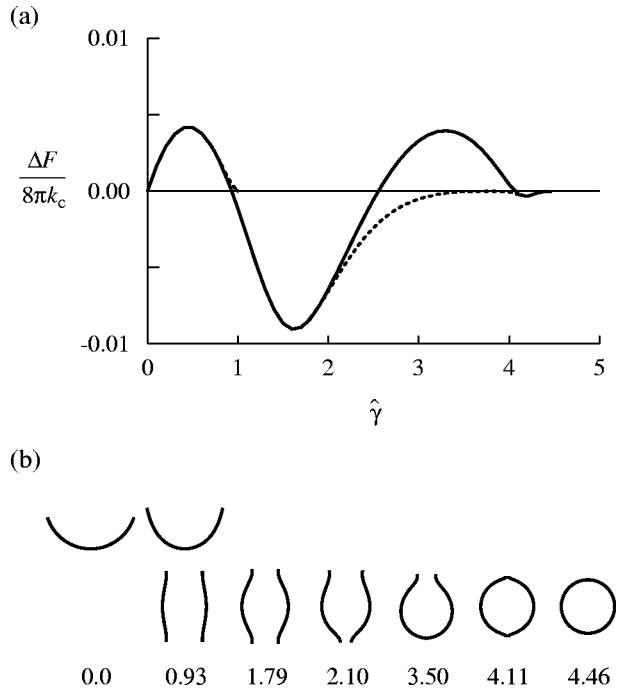

FIG. 4. The deformation of opening-up surfaces when $m_0/4\pi = 0.72$. (a) Relative energies of tube and funnel to cup shapes as functions of $\hat{\gamma}$. Solid line represents $(F_{\text{tube}}-F_{\text{cup}})/8\pi k_c$ and dotted line shows $(F_{\text{funnel}}-F_{\text{cup}})/8\pi k_c$. (b) Stable shapes at the indicated values of $\hat{\gamma}$.

$\hat{\gamma}=2.0$, in which two infinitesimal holes open in a spherical surface. As $\hat{\gamma}$ decreases, the holes expand and the entire shape becomes a short tube. The energy–line-tension graph does not fold and the energy is always lower than that of a sphere for $0<\hat{\gamma}<2.0$. Therefore, a continuous transition between the sphere and the tube occurs at $\hat{\gamma}=2.0$.

In the case of the intermediate values of m_0, the energies of cups and tubes become very close, and the third type of shape emerges, in which the two holes of a tube have different sizes. We call this shape a funnel. When $m_0/4\pi=0.72$, the shape of the lowest energy turns out to be a cup, a tube, or a funnel according to $\hat{\gamma}$ (Fig. 4). The funnel bifurcates from the tube at $\hat{\gamma}=1.79$ and the two holes decrease their size unequally as $\hat{\gamma}$ increases. At $\hat{\gamma}=3.5$, one of the holes becomes very small and the entire shape is like a cup. Then the other hole shrinks and the shape transforms to a tube again at $\hat{\gamma}=4.11$. Although funnel shapes also emerge for $0.71<\hat{\gamma}<0.80$, they have higher energy than the cups and the tubes with the same $\hat{\gamma}$. This suggests that the funnel is unstable and that stable cups and tubes coexist in this region.

D. Phase diagram

To obtain the phase diagram for opening-up surfaces, we compared the energy F of the cup, tube, funnel, and sphere. Figure 5 shows the shape of the lowest energy for given m_0 and $\hat{\gamma}$. Note that this diagram is incomplete, because the nonaxisymmetric shape is not taken into consideration.

In general, opening-up shapes emerge when $\hat{\gamma}$ are small, but the conditions for hole openings and membrane shapes also depend on m_0. In particular, for $m_0/4\pi>1.23$ no opening-up shape was found. The critical m_0 corresponds to $c_0=(\hat{k}_r/2)(m_0-4\pi)=2.0$ for the sphere, suggesting that $c_0<2$ is a condition for a spherical membrane to open holes. Within the range $m_0/4\pi<1.23$, larger m_0 tends to stabilize tube shapes, whereas small m_0 is favorable for cup shapes. Funnel shapes are realized for intermediate m_0. In the cup-shape region, there is a small domain D where no cup shape was found. What shapes are realized in this region is unknown, for nonaxisymmetric shapes may exist. The transition between the sphere and the tube shapes is continuous, while it is discontinuous between the sphere and the cup shapes. Numerical calculation showed that the continuous transition occurs at $\hat{\gamma}=2-c_0$.

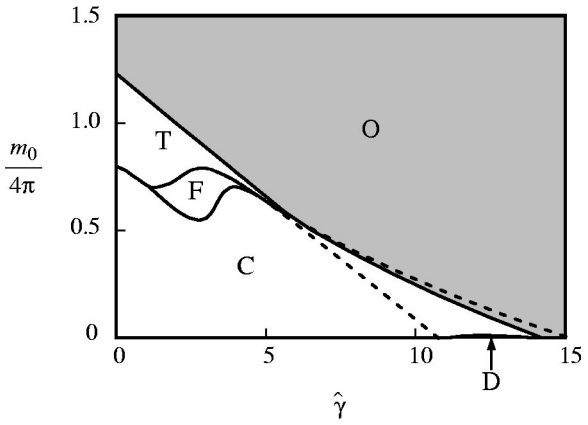

FIG. 5. Phase diagram of opening-up surfaces for $\hat{k}_r=1.4$ and $\hat{k}_g=0$. The shape of the lowest energy for given m_0 and $\hat{\gamma}$ is shown. *O*, sphere; *T*, tube; *F*, funnel; and *C*, cup. In domain *D*, no cup shape was found. Dashed lines represent the region of bistability between a cup and a sphere.

Opening-up shapes with $\hat{\gamma}=0$ have a striking feature. When $\hat{\gamma}=0$ and $\hat{k}_g=0$, all the surfaces satisfying $H=c_0/2$ are the solution of Eq. (9) and the boundary conditions (11)–(13) if $\lambda=c_0^2/2$. From Eqs. (6) and (10), c_0 is given by $c_0=\hat{k}_r m_0/2(1+\pi\hat{k}_r)$. The shapes depicted in Figs. 1–3 at $\hat{\gamma}=0$ are examples of such surfaces. Even in the axisymmetric case, there exist an infinite number of shapes for a given constant mean curvature. In addition, there also exist an infinite number of nonaxisymmetric shapes, and, furthermore, all these surfaces have the same energy $\hat{F}=\hat{k}_r m_0^2/2(1+\pi\hat{k}_r)$. Therefore, the surface shape cannot be uniquely determined when $\hat{\gamma}=0$. In that case, membranes are expected to be very flexible and their shape fluctuates thermally.

E. The effect of the Gaussian bending modulus

The equilibrium shape of closed vesicles is considered to be independent of the Gaussian curvature modulus k_g, because the surface integral of the Gaussian curvature K has the same constant value for any closed surface of the same topology. For an opening-up vesicle, on the other hand, the surface integral of K depends on the surface shape in general, and the equilibrium shape may be affected by the Gaussian curvature modulus.

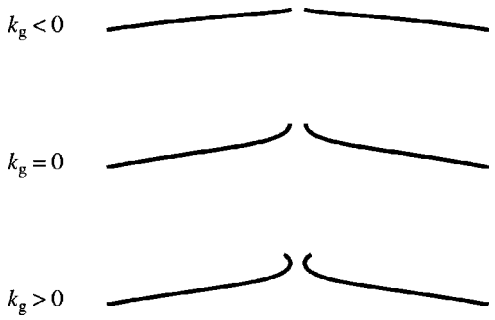

FIG. 6. Schematic diagram of the shape of a small hole opening in a nearly spherical surface. The shape of the rim varies according to k_g.

Numerical calculations showed that k_g has little effect on the surface shape when holes largely open in the surface. However, if the hole size is small the surface shape is greatly affected by k_g (Fig. 6). When $k_g<0$, the surface is relatively flat in the vicinity of the hole. As the hole size reduces, the surface closes smoothly and the nondimensional line tension $\hat{\gamma}$ shrinks to zero. On the other hand, when $k_g=0$ the membrane around the hole is protruded to form a volcanolike shape. As the hole size decreases, the volcano becomes smaller but steeper. In the limit of the infinitesimal hole, the surface becomes parallel to the axis of rotation at the lip of the volcano, and $\hat{\gamma}$ converges to $2-c_0=2-(\hat{k}_r/2)(m_0-4\pi)$. When $k_g>0$, the surface is more protruded and the lip is curled up. The hole never closes because the neck is infinitesimally narrowed before the lip is sealed. Similar transformations of the hole shape with nonzero k_g are seen in the surfaces with two holes.

These results indicate that if small holes are found in vesicles, we may evaluate the value (or at least the sign) of the Gaussian bending modulus by observing the hole shape. Although one of the authors predicted a small value of the Gaussian bending modulus for liquid membranes [19], the precise observation of the opening-up vesicle will clarify the validity of the theory.

F. Membranes without nonlocal bending energy

So far, we have assumed the relaxed area difference ΔA_0 to be fixed. However, when a membrane has a hole, the lipids may possibly migrate across the edge of the hole from one monolayer to the other. Then ΔA_0 will be adapted to the actual area difference ΔA which is determined by the vesicle shape. To investigate this effect, we calculated the vesicle shape using a minimal model in which the nonlocal bending energy is completely relaxed.

Figure 7 shows the shape change of opening-up vesicles when $\Delta A_0=\Delta A$ and $k_g=0$. In this case, a disk with the radius $2R_0$ is always a solution of Eq. (9) with the boundary conditions. The energy of the disk ($4\pi R_0\gamma$) is smaller than that of a spherical vesicle ($8\pi k_c$) when $\hat{\gamma}<2$. The energy–line-tension graph of cup-shaped solutions has two branches. On the lower branch, cup shapes bifurcate from a sphere at $\hat{\gamma}=2.00$ and the hole expands as $\hat{\gamma}$ decreases to 1.52. On the upper branch, the size of the hole increases with $\hat{\gamma}$ and the

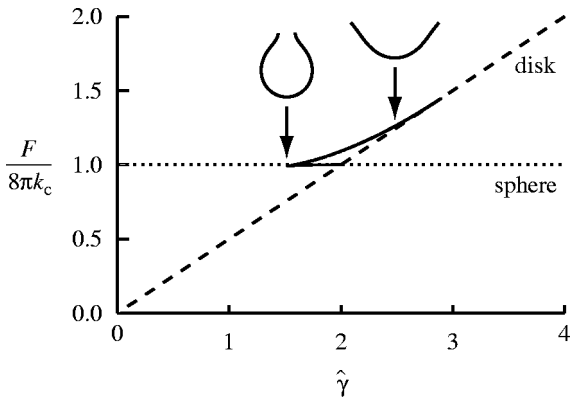

FIG. 7. Shape transformations of vesicles predicted by the minimal model. Energy of a sphere (dotted line) or that of a disk (dashed line) is lower than the energy of cup shapes (solid line).

cup finally becomes a disk at $\hat{\gamma}=2.89$. Cup shapes on the lower branch have lower energy than the sphere, which suggests that they are locally stable. However, their energy is much higher than that of a disk. Although equilibrium surfaces with two holes also exist (not shown), they have higher energy than the disk as well. Therefore, spherical vesicles are expected to transform discontinuously to a disk-shaped membrane sheet when $\hat{\gamma}$ decreases below 2. Conversely, a disk becomes a sphere when $\hat{\gamma}$ increases to more than 2.

IV. EXPERIMENTALLY OBSERVED SHAPES

The observation by Saitoh *et al.* [2] showed that the protein talin induces opening-up vesicles with both one hole and multiple holes (Fig. 8). As to the vesicles with single hole, the transition to the cup shape seemed to be discontinuous since no intermediate shape between the cup and the sphere was found. Once a hole opened, the vesicle shape largely depended on the concentration of talin. Though cup-shaped vesicles were observed at low concentration, the hole size became larger with increasing concentration and the cups transformed into a dish shape [Figs. 8(a)–8(c)]. Conversely,

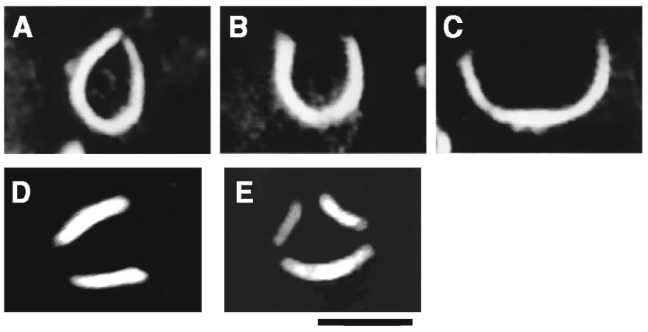

FIG. 8. Opening-up vesicles observed by dark-field microscopy in the presence of talin (photographs are taken from Figs. 1, 3, and 4 in Saitoh *et al.* [2]). (a)–(c) A sequence of photographs showing morphological changes of a vesicle at talin concentrations vary from 0 to 2 μM. (d) A vesicle with two holes observed in the presence of 1 μM talin. (e) A vesicle with three holes observed in the presence of 1.5 μM talin. (Bar=5 μm.)

diluting the talin caused the cup-shaped membranes to transform into the original spherical vesicles. These observations well agree with the result shown in Fig. 2, since the effective line tension depends on the talin concentration [12]. When the talin concentration was further increased, the vesicles became a flexible sheet whose shape fluctuated greatly. The exact morphology of sheet-shaped membranes could not be evaluated by dark-field microscopy, while the theoretical results suggest a surface with a constant mean curvature.

The fact that the calculations shown in Fig. 2 reproduce the actual transformations of opening-up vesicles indicates that the membranes maintained the value of ΔA_0. If lipids could easily migrate across the hole edge from one monolayer to the other, as stated in Sec. III F, ΔA_0 would be rapidly relaxed, and direct transformation would take place between the sphere and the sheet. Talin is a high-molecular-weight protein (200 kDa). Moreover, fluorescent micrographs showed that talin was localized mainly along the membrane edges [2]. Talin molecules may accumulate at the edges of holes and prevent the migration of lipids between the layers.

Opening-up vesicles with multiple holes were observed when the concentration of talin was abruptly increased. Funnel-shape vesicles were frequently observed and vesicles with three holes were also found with a high concentration of talin [Figs. 8(d) and 8(e)]. The fact that the opening of multiple holes required a high concentration of talin (i.e., low γ) corresponds with the theoretical phase diagram shown in Fig. 5. However, for some unexplained reason, only cup-shaped vesicles were obtained when the talin concentration was gradually increased. Therefore, it is unclear whether the transition between the sphere and the multiple-hole vesicles is continuous or not. In addition, we could not find small holes in the membrane to evaluate the Gaussian bending modulus. It is unknown why tube shapes, which are predicted for small γ and large m_0, were rarely found in the experiment. Some of the experimental conditions may have had the effect of reducing the m_0 of membranes, or another possibility is that most of the tube shapes calculated for small γ and large m_0 are actually unstable for a nonaxisymmetric deformation, and shapes having more than two holes are realized for these parameters. To draw more definite conclusions, further studies will be needed both theoretically and experimentally.

Cup-shaped vesicles have also been observed when detergents are applied [3]. The observations showed that, like vesicles with increasing talin concentration, spherical vesicles transformed discontinuously to a cup and then gradually unfolded to become a sheet. In this case, the membrane area continuously decreased due to the solubilization of lipids by detergents, and the reduction of $\hat{\gamma}=\gamma R_0/k_c$ with R_0 may be the cause of the shape transformations. Although the area reduction rates are not always the same between the two monolayers of opening-up vesicles, m_0 may have remained almost steady for a short time. In case of the transformations by detergents, no multiple-hole vesicles were found. This can be understood through the reduction of m_0, since the detergents may extract lipid molecules mainly from the outer leaflet of the membranes and reduce the area. In some combinations of detergents and lipid molecules, it has been reported that inside-out inversion of membranes took place after the opening up of a hole [3]. A greater reduction of the area of the outer leaflet by detergents may produce a negative m_0, causing an inverse rapid bend of the membranes.

We now give a rough estimation of the line tension for opening-up vesicles. Although the critical line tension for hole opening depends on m_0, Fig. 5 indicates that opening-up vesicles are formed when $\hat{\gamma}$ is smaller than 14. Using typical values $k_c \approx 10^{-19}$ J and $R_0 \approx 1$ μm gives the critical line tension as $\gamma_c < 1.4$ pN, which is considerably lower than the traditional value ~ 10 pN [20]. Therefore, we can conclude that chemical agents such as talin and detergents reduce the line tension by a factor of $10-10^2$ compared with membranes without additive components. There are no reliable data for membranes with talin, but the line tension with detergents has been estimated by measuring the duration time of transient membrane holes [21] or the magnitudes of membrane fluctuations [22]; both estimations showed that the line tension is on the order of 0.1 pN. This value is in reasonable agreement with our theoretical estimation.

V. CONCLUSIONS

In this paper, we analyzed the shapes of opening-up vesicles by taking into account the line tension of membrane holes and the bending energy of membranes, using the area difference elasticity model. We formulated the Euler-Lagrange equation and the boundary conditions holding on the membrane edge, and numerically solved them to obtain axisymmetric vesicle shapes that minimize the total energy. Numerical results showed that when the line tension is very low, opening-up vesicles may have lower energy than closed spherical ones so that large, stable holes open in the vesicles. However, the relaxed area difference between the two monolayers of bilayer membranes is also an important factor for stabilizing the opening-up vesicles. Depending on the values of the line tension and the relaxed area difference, the model gives cup-, funnel-, and tube-shaped vesicles. The calculated shapes and the phase diagram well agree with the shape transformations of opening-up vesicles observed when the protein talin or some detergents were added, indicating that the line tension of the membrane is greatly reduced by these additive molecules.

We also showed that the Gaussian bending modulus affects the vesicle shape when the size of the membrane hole is small. Since the shape of closed vesicles is independent of the Gaussian bending modulus, its estimation has been considered to require the measurement of the energy change for the fusion or fission of vesicles. However, our finding may provide another way to detect the Gaussian curvature modulus by observing opening-up vesicles. Although our results showed that cup shapes with a small hole are mostly unstable, it is possible that we may find small, stable holes in multiple-hole vesicles. There may be other indications besides the shape of small holes to distinguish the Gaussian curvature modulus. To develop a method to measure the Gaussian bending modulus is an interesting task for future study.

In the present work, we have analyzed only axisymmetric shapes. However, some nonaxisymmetric shapes, such as a

vesicle with three holes, have been observed in experiments. Analysis of nonaxisymmetric shapes will be a future work to obtain a complete phase diagram. To evaluate the thermal fluctuations of membranes and membrane holes is another important problem. Recent studies have shown that opening-up vesicles are induced by proteins other than talin. Moreover, proteins and detergents have the ability to stimulate various topological transformations of vesicles including membrane fusion [23]. Approaches, such as used in this current analysis, will also be useful in obtaining a better understanding of these phenomena.

ACKNOWLEDGMENT

This work was partly supported by Grants-in-Aid for Scientific Research (C) from the Japan Society for the Promotion of Science.

APPENDIX A: AXISYMMETRIC SHAPES

We consider the case that the surface Σ is an axisymmetric shape. By parametrizing the surface shape with the arclength t of the contour and the azimuthal angle ϕ, we represent the point vector of the surface as

$$\mathbf{p}(t,\phi) = r(t)\cos\phi\hat{\mathbf{i}} + r(t)\sin\phi\hat{\mathbf{j}} + z(t)\hat{\mathbf{k}}. \tag{A1}$$

We introduce a function $\psi(t)$ which represents the angle of the contour. ψ is related to r and z by

$$\dot{r} = \cos\psi \quad \text{and} \quad \dot{z} = \sin\psi, \tag{A2}$$

respectively, while the overdot denotes a derivative with respect to t. Then the curvatures are given by

$$H = \frac{1}{2}\left(\dot{\psi} + \frac{\sin\psi}{r}\right), \quad K = \frac{\dot{\psi}\sin\psi}{r},$$

$$c_n = \frac{\sin\psi}{r}, \quad c_g = \frac{\cos\psi}{r}, \quad \tau = 0, \tag{A3}$$

and the shape equation (9) becomes

$$\frac{1}{r}\frac{d}{dt}(r\dot{H}) + 2H(H^2 - K) + c_0 K - \lambda H = 0. \tag{A4}$$

The boundary conditions at $t=0$ are

$$r(0) = z(0) = \psi(0) = 0, \tag{A5}$$

since the surface is smooth on the z axis. At $t=t_0$, the following boundary conditions follow from Eqs. (11)–(13) and (A3):

$$2\dot{H} + \hat{\gamma}\frac{\sin\psi}{r} = 0, \tag{A6}$$

$$2H - c_0 + \hat{k}_g\frac{\sin\psi}{r} = 0, \tag{A7}$$

$$2H(H - c_0) + \hat{k}_g K + \lambda + \hat{\gamma}\frac{\cos\psi}{r} = 0. \tag{A8}$$

If we multiply Eq. (A4) by $r\cos\psi$, integrate it with t, divide it by $r\cos\psi$, and use Eqs. (A6)–(A8), we have

$$2\dot{H} - \frac{\sin\psi}{r}N = 0, \tag{A9}$$

where

$$N = \frac{r}{\cos\psi}\left[-H\left(\dot{\psi} - \frac{\sin\psi}{r}\right) - c_0\frac{\sin\psi}{r} + \lambda\right]. \tag{A10}$$

Differentiating Eq. (A10) gives

$$\dot{N} = \frac{\cos\psi}{r}N + (2H - c_0)\left(\dot{\psi} - \frac{\sin\psi}{r}\right). \tag{A11}$$

Equations (A9) and (A11) are convenient for numerical calculations.

APPENDIX B: NUMERICAL METHOD

To get precision in the numerical integration, we introduce an independent variable

$$\tau = (1/L)\int_0^t (1 + \dot{\psi}^2)^{1/2} dt, \tag{B1}$$

where L is a constant determined by $\tau(t_0)=1$. To calculate $m=\int_\Sigma H\,dA$ and the area constraint $A=4\pi$, we define two functions

$$a(t) = \int_0^t r\,dt \tag{B2}$$

and

$$\mu(t) = \int_0^t Hr\,dt. \tag{B3}$$

Then from Eqs. (A2), (A3), (A9), (A11), (B2), and (B3), we have the following set of ordinary differential equations:

$$H' = \frac{\Psi N\sin\psi}{2r},$$

$$N' = \Psi\left[\frac{\cos\psi}{r}N + 2(2H - c_0)\left(H - \frac{\sin\psi}{r}\right)\right],$$

$$\psi' = \Psi\left[2H - \frac{\sin\psi}{r}\right], \quad r' = \Psi\cos\psi,$$

$$z' = \Psi\sin\psi, \quad a' = \Psi r, \quad \mu' = \Psi Hr, \quad c_0' = 0, \quad L' = 0, \tag{B4}$$

where the prime represents $d/d\tau$ and

$$\Psi = L[1 + (2H - \sin\psi/r)^2]^{-1/2}. \quad \text{(B5)}$$

Equations (10) and (A6)–(A8) and the area constraint give the following boundary conditions:

$$r(0) = z(0) = \psi(0) = a(0) = \mu(0) = 0,$$

$$a(1) = 2, \quad \mu(1) = (m_0 - 2c_0/\hat{k}_r)/2\pi,$$

$$H(1) = \frac{1}{2}\left[c_0 - \hat{k}_g \frac{\sin\psi}{r}\right], \quad N(1) = -\hat{\gamma}. \quad \text{(B6)}$$

In a case where there are two holes on the both ends of the surface, the conditions

$$H(0) = \frac{1}{2}\left[c_0 - \hat{k}_g \frac{\sin\psi}{r}\right], \quad N(0) = \hat{\gamma} \quad \text{(B7)}$$

replace $r(0)=0$ and $\psi(0)=0$. We solved Eqs. (B4) with the conditions (B6) or (B7) using the relaxation method [24].

[1] U. Seifert and R. Lipowsky, in *Structure and Dynamics of Membranes*, edited by R. Lipowsky and E. Sackmann (Elsevier Science, Amsterdam, 1995), p. 403.
[2] A. Saitoh, K. Takiguchi, Y. Tanaka, and H. Hotani, Proc. Natl. Acad. Sci. U.S.A. **95**, 1026 (1998).
[3] F. Nomura, M. Nagata, T. Inaba, H. Hiramatsu, H. Hotani, and K. Takiguchi, Proc. Natl. Acad. Sci. U.S.A. **98**, 2340 (2001).
[4] C. E. Dempsey, Biochim. Biophys. Acta **1031**, 143 (1990).
[5] D. V. Zhelev and D. Needham, Biochim. Biophys. Acta **1147**, 89 (1993).
[6] P. G. de Gennes and C. Tauppin, J. Phys. Chem. **86**, 2294 (1982).
[7] R. Bar-Ziv, T. Frisch, and E. Moses, Phys. Rev. Lett. **75**, 3481 (1995).
[8] O. Sandre, L. Moreaux, and F. Brochard-Wyart, Proc. Natl. Acad. Sci. U.S.A. **96**, 10591 (1999).
[9] J. D. Moroz and P. Nelson, Biophys. J. **72**, 2212 (1997).
[10] F. Brochard-Wyart, P. G. de Gennes, and O. Sandre, Physica A **278**, 32 (2000).
[11] H. Isambert, Phys. Rev. Lett. **80**, 3404 (1998); M. D. Betterton and M. P. Brenner, *ibid.* **82**, 1598 (1999).
[12] Y. Suezaki, H. Ichinose, K. Takiguchi, and H. Hotani, Biophys. Chem. **80**, 119 (1999).
[13] W. Helfrich, Z. Naturforsch. C **28**, 693 (1973).
[14] L. Miao, U. Seifert, M. Wortis, and H.-G. Dŏbereiner, Phys. Rev. E **49**, 5389 (1994).
[15] Z. C. Tu and Z. C. Ou-Yang, Phys. Rev. E **68**, 061915 (2003).
[16] R. E. Waugh, J. Song, S. Svetina, and B. Zeks, Biophys. J. **61**, 974 (1992).
[17] Z. C. Ou-Yang and W. Helfrich, Phys. Rev. A **39**, 5280 (1989).
[18] M. Jarić, U. Seifert, W. Wintz, and M. Wortis, Phys. Rev. E **52**, 6623 (1995).
[19] Y. Suezaki and H. Ichinose, J. Phys. I **5**, 1469 (1995).
[20] E. Evans, V. Heinrich, F. Ludwig, and W. Rawicz, Biophys. J. **85**, 2342 (2003).
[21] E. Karatekin, O. Sandre, H. Guitouni, N. Borghi, P.-H. Puech, and F. Brochard-Wyart, Biophys. J. **84**, 1734 (2003).
[22] T. Umeda, F. Nomura, T. Inaba, K. Takiguchi, and H. Hotani (unpublished).
[23] K. Takiguchi, F. Nomura, T. Inaba, S. Takeda, A. Saitoh, and H. Hotani, ChemPhysChem **3**, 571 (2002).
[24] W. H. Press, S. A. Teukolsky, W. T. Vetterling, and B. P. Flannery, *Numerical Recipes in C* (Cambridge University Press, Cambridge, U.K., 1988).